Supplement of Atmos. Chem. Phys., 16, 2785–2802, 2016
http://www.atmos-chem-phys.net/16/2785/2016/
doi:10.5194/acp-16-2785-2016-supplement

Atmospheric Chemistry and Physics Open Access EGU

Supplement of

SOA formation from the photooxidation of α-pinene: systematic exploration of the simulation of chamber data

Renee C. McVay et al.

Correspondence to: John H. Seinfeld (seinfeld@caltech.edu)

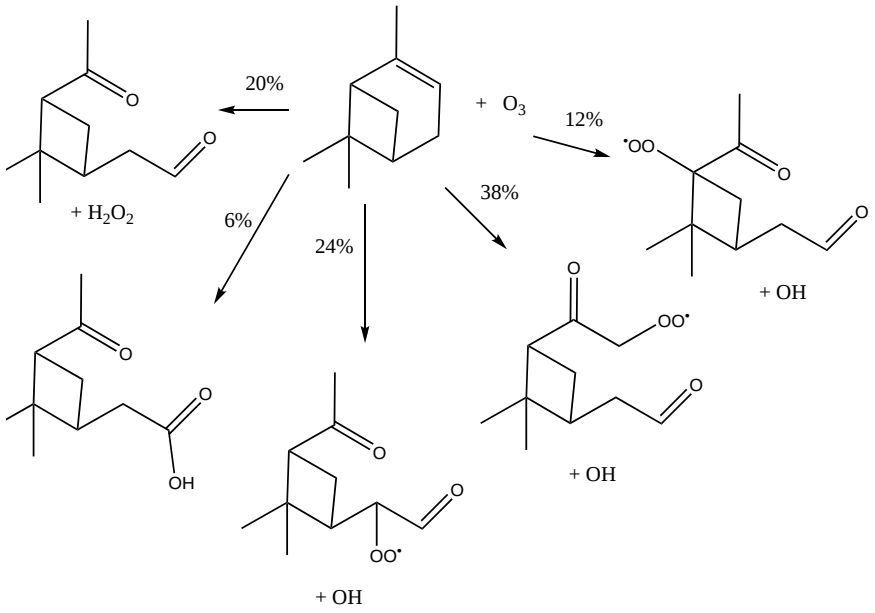

Figure S1: Overview of the α-pinene + O_3 initial reaction step in GECKO-A. All subsequent chemistry is generated according to the standard protocols in GECKO-A.

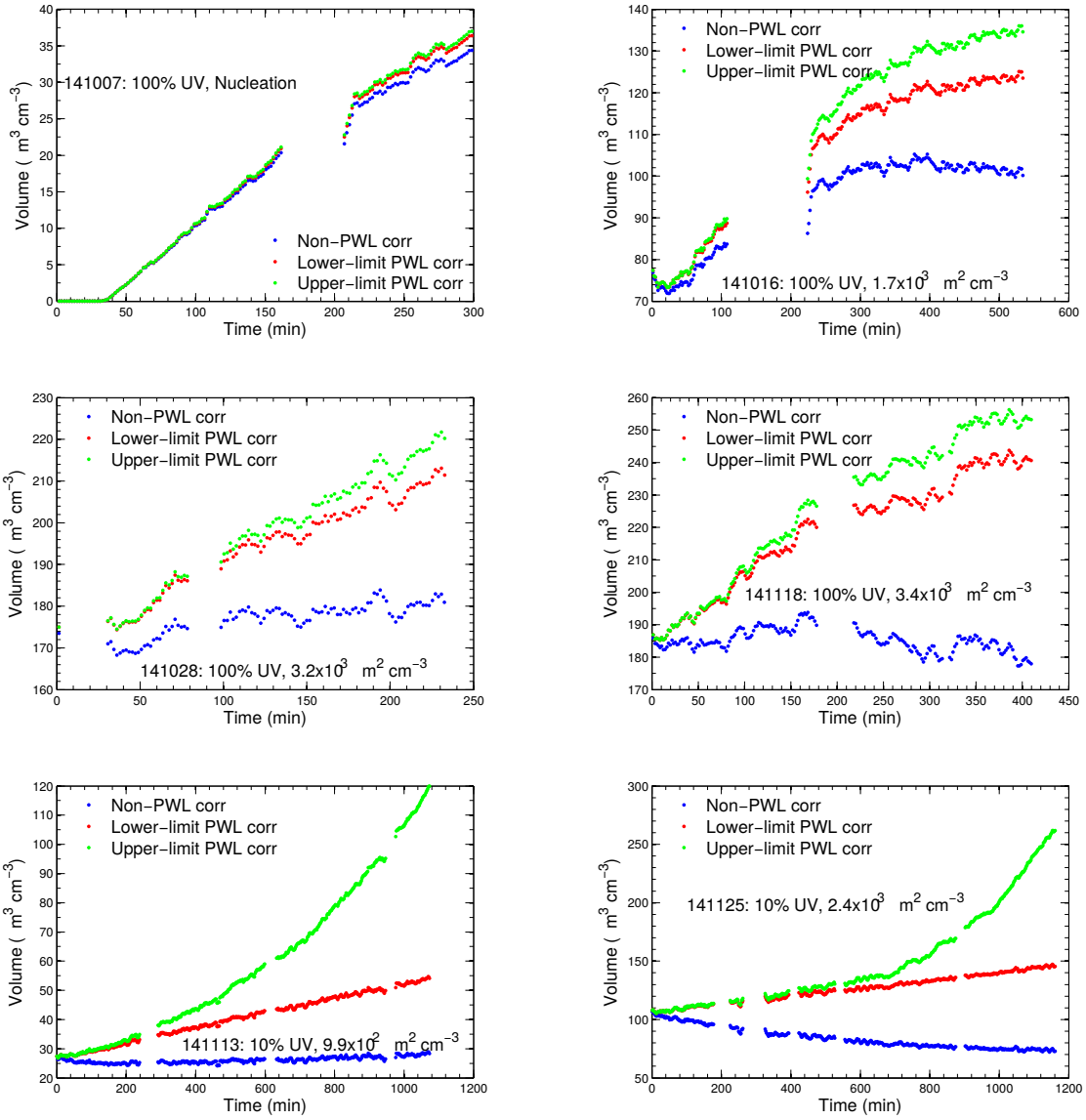

Figure S2: Caption on next page.

Figure S2: Total particle volume as a function of time, non-particle wall loss corrected (blue data points) and using two different corrections for particle wall loss. Red data points have been corrected with the lower bound assumption, in which deposited particles are assumed to not interact with vapor, and the mass of SOA present on a particle at the moment of its deposition is added to the total SOA. Green data points have been corrected with the upper bound assumption, in which deposited particles continue to grow via condensation at the same rate as suspended particles. The dramatic increase in the upper bound towards the end of the low UV experiments is likely an artifact of how the upper bound is calculated. The Aerosol Parameter Model (Pierce et al., 2008) is used to constrain the rate of condensation to particles by fitting the DMA size distribution at each time step, and this condensation rate is then applied to deposited particles. At the end of the low UV experiments, only 11% of the initial total number of particles remain suspended, as opposed to 30-40% for the high UV experiments. SOA growth in the α-pinene system is not seed surface area dependent (discussed in the Results section), and condensation to suspended particles will not decrease due to the decreased number. Therefore, at the end of the low UV experiments, the condensation rate per suspended particle is very large. With the upper bound correction, the deposited particles then grow with the same high condensation rate, despite the fact that transport to deposited particles will be slower than transport to suspended particles. The upper bound is likely a substantial overestimation for these experiments.

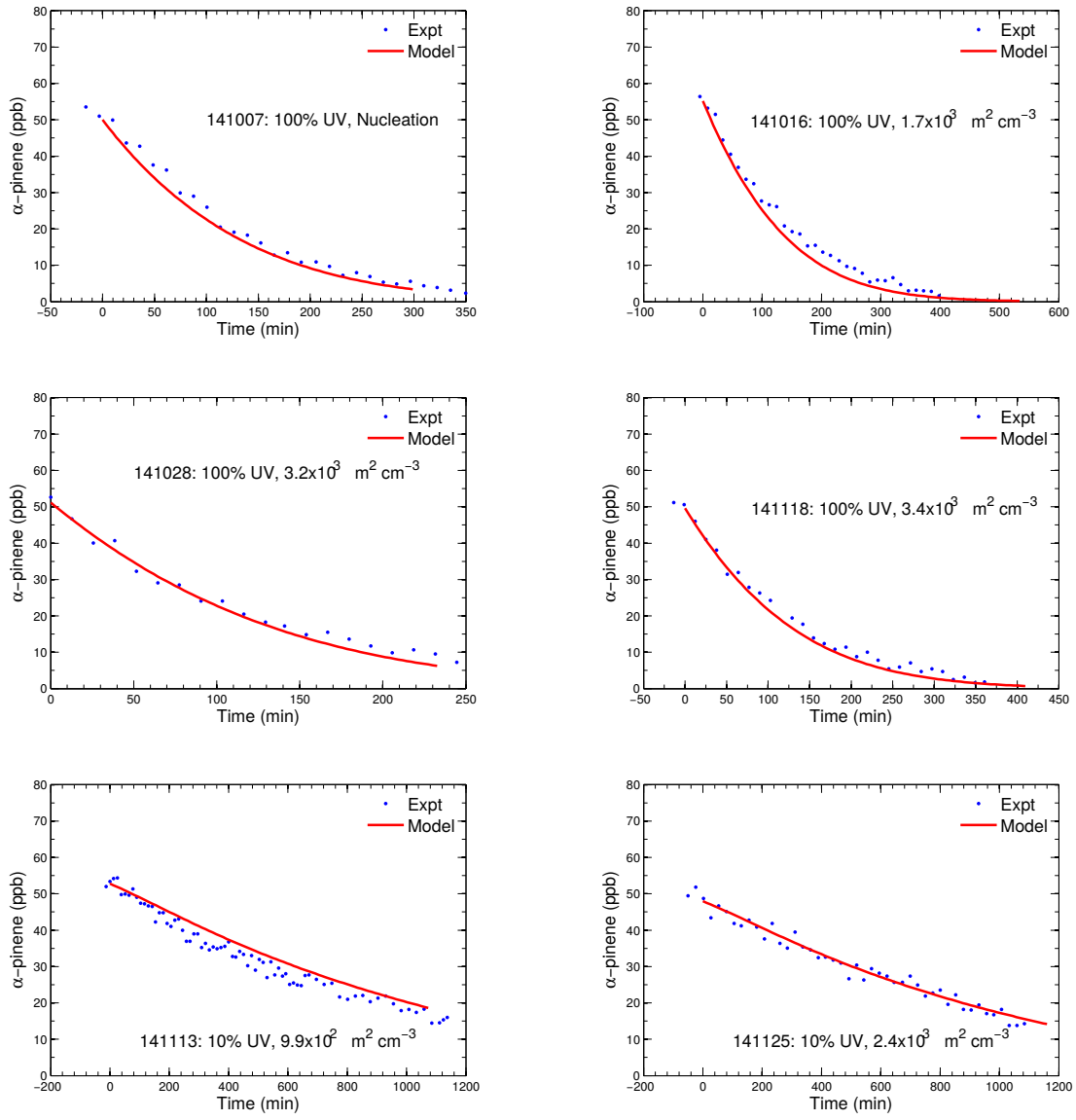

Figure S3: Decay of α-pinene as a function of time for the six different photooxidation experiments. Experimental datapoints are shown with blue data points, and GECKO-A predictions are shown with solid red lines.

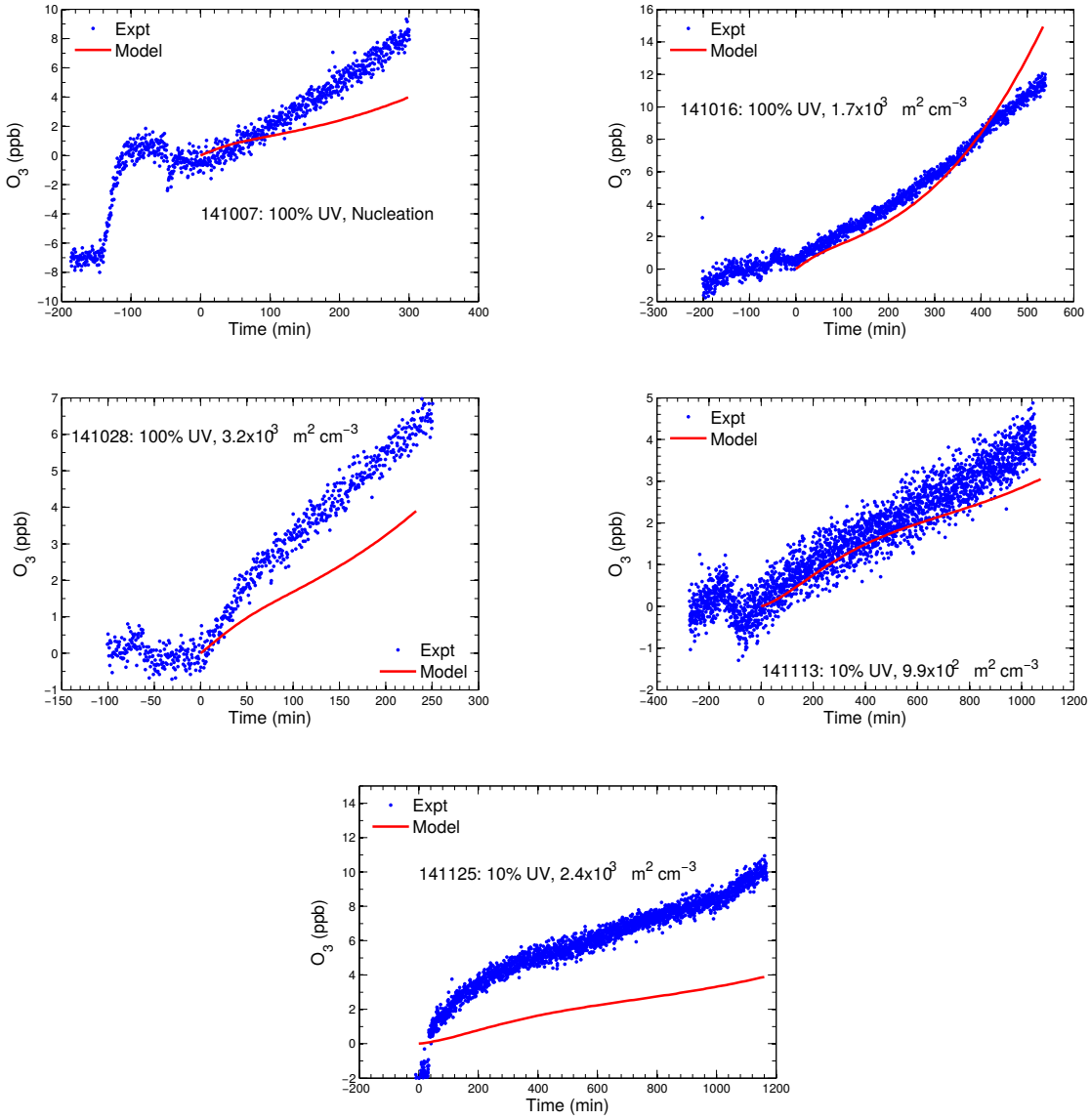

Figure S4: O_3 formation as a function of time for five of the six experiments. The O_3 analyzer malfunctioned during one of the experiments (not shown). Because α-pinene was not observed to decay before lights were turned on, the initial O_3 concentration was assumed to be zero. Therefore, the experimental O_3 measurements have been normalized to the measured value at time zero (lights on). A NO_x wall off-gassing rate of 2.5 ppt min^{-1} was optimized to match the observed O_3 formation. Although predicted O_3 concentrations do not correspond exactly to O_3 observations, SOA was not affected by changing the NO_x wall off-gassing rate.

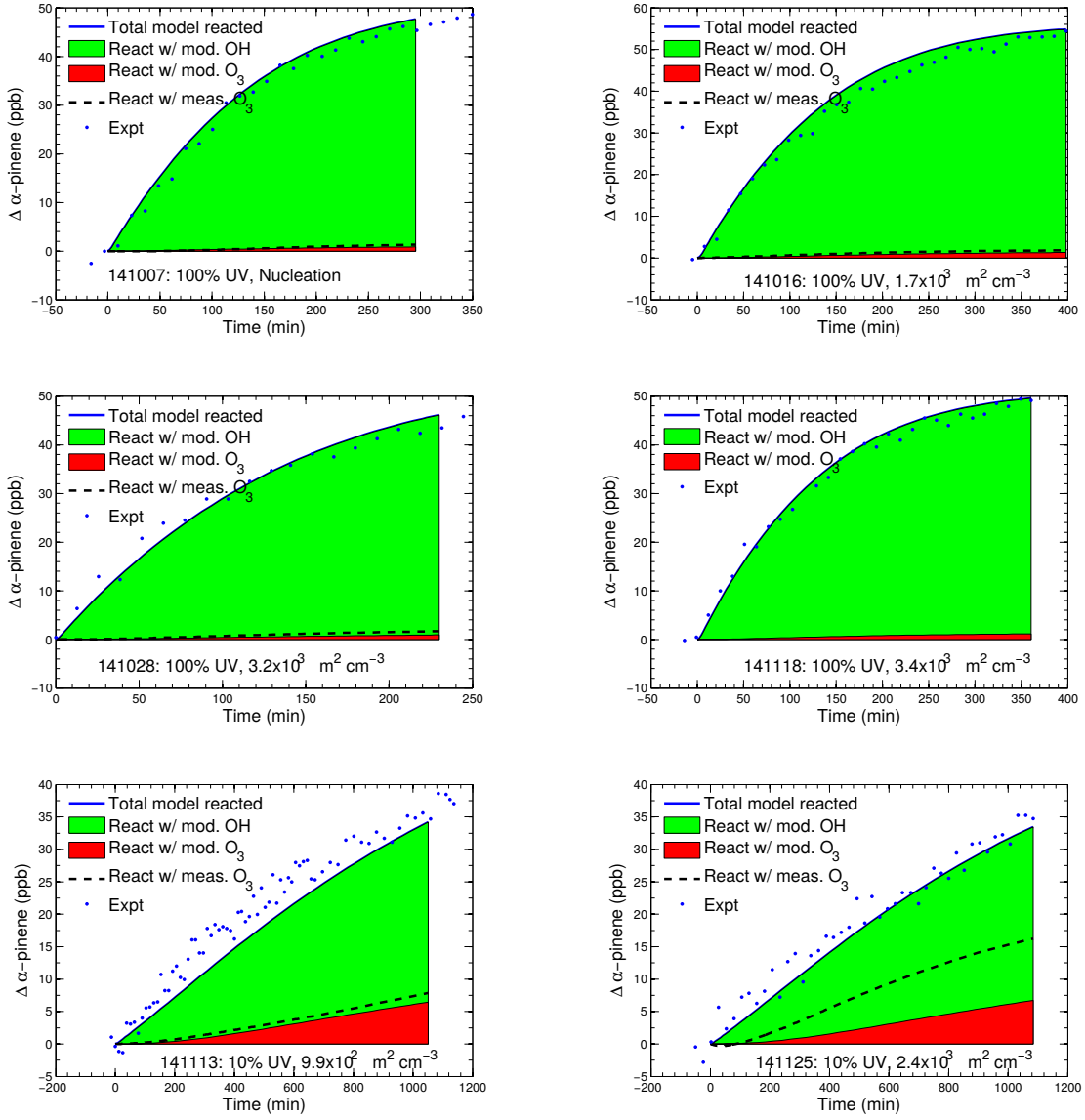

Figure S5: Amount of α-pinene predicted to be reacted with OH versus O_3, for both modeled and measured O_3 concentrations. The solid blue line shows the total α-pinene reacted. The green area shows the amount reacted with OH based on the modeled OH concentration. The red area shows the amount reacted with O_3 based on the modeled O_3 concentration. The dashed black line shows the amount predicted to have reacted with the measured O_3 concentration. Because the O_3 monitor malfunctioned during experiment 141118, the dashed line is not shown for this experiment.

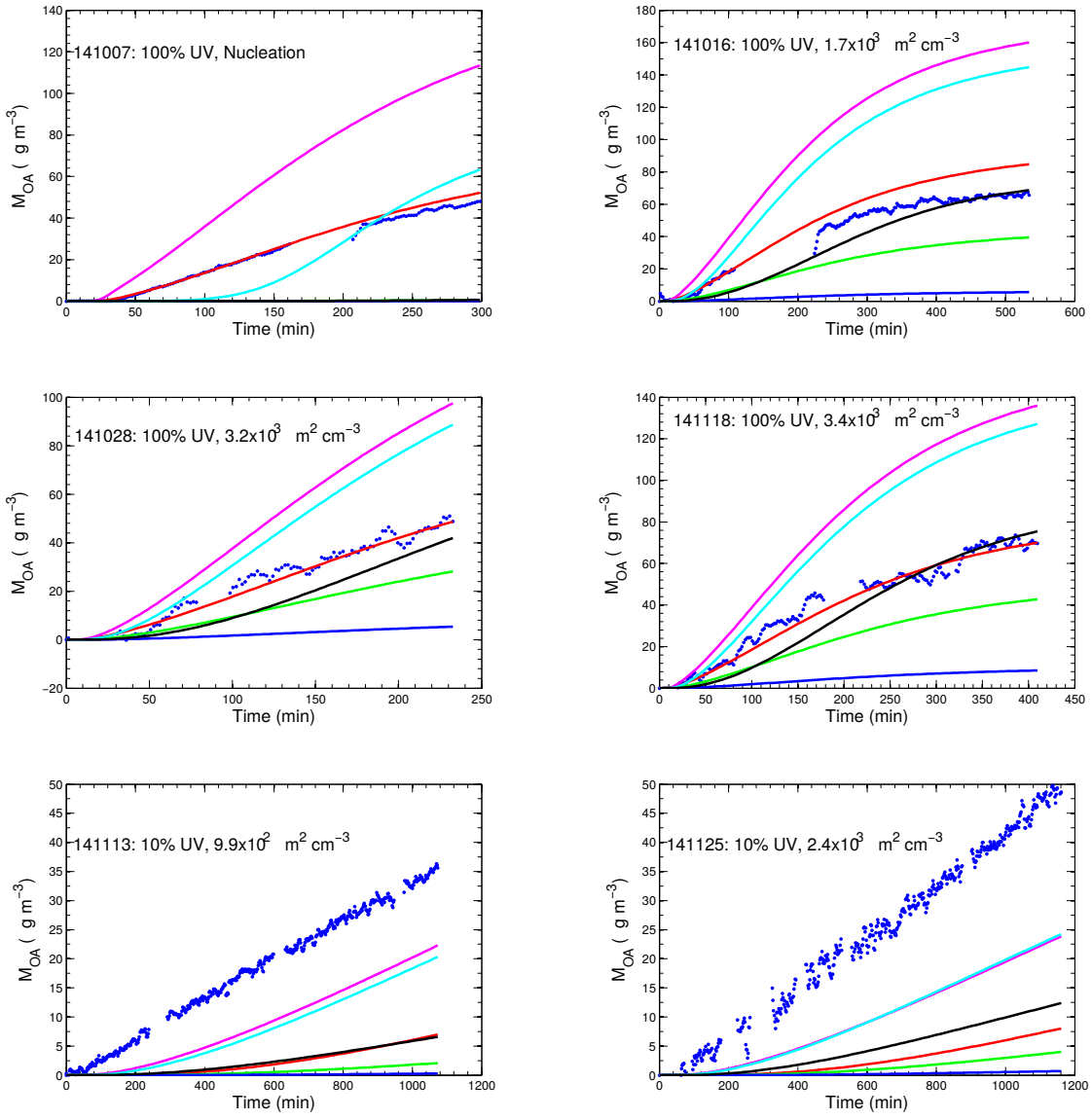

Figure S6: Caption on next page.

Figure S6: Mass of organic aerosol as a function of time. Experimental measurements are shown with blue data points. GECKO-A predictions are shown for different combinations of the vapor-particle accommodation coefficient α_p and the vapor-wall loss rate k_{gw}: Red line: α_p=1 and $k_{gw} = 10^{-3}$ s^{-1}; green line: α_p=0.01 and $k_{gw} = 10^{-3}$ s^{-1}; blue line: α_p=0.001 and $k_{gw} = 10^{-3}$ s^{-1}; pink line: α_p=1 and $k_{gw} = 10^{-4}$ s^{-1}; cyan line: α_p=0.01 and $k_{gw} = 10^{-4}$ s^{-1}; black line: α_p=0.001 and $k_{gw} = 10^{-4}$ s^{-1}. α_p=0.1 is not shown; this value gives almost identical predictions to α_p=1 with the exception of the nucleation experiment, in which significantly less SOA is predicted. For the 100% UV experiments, decreasing α_p delays the onset of SOA formation which is not consistent with the observations. Lowering the wall loss rate to 10^{-4} s^{-1} for the 100% UV experiments results in significant overprediction of SOA for all α_p except $\alpha_p = 0.001$. Although this combination yields an ending SOA similar to that of the experiment, the shape of the curve does not agree with experimental observations. Based on these sensitivity tests, $\alpha_p = 1$ and $k_{gw} = 10^{-3}$ s^{-1} were determined to provide the best fit for the 100% UV experiments. All of the combinations shown result in significant underprediction for the 10% UV experiments.

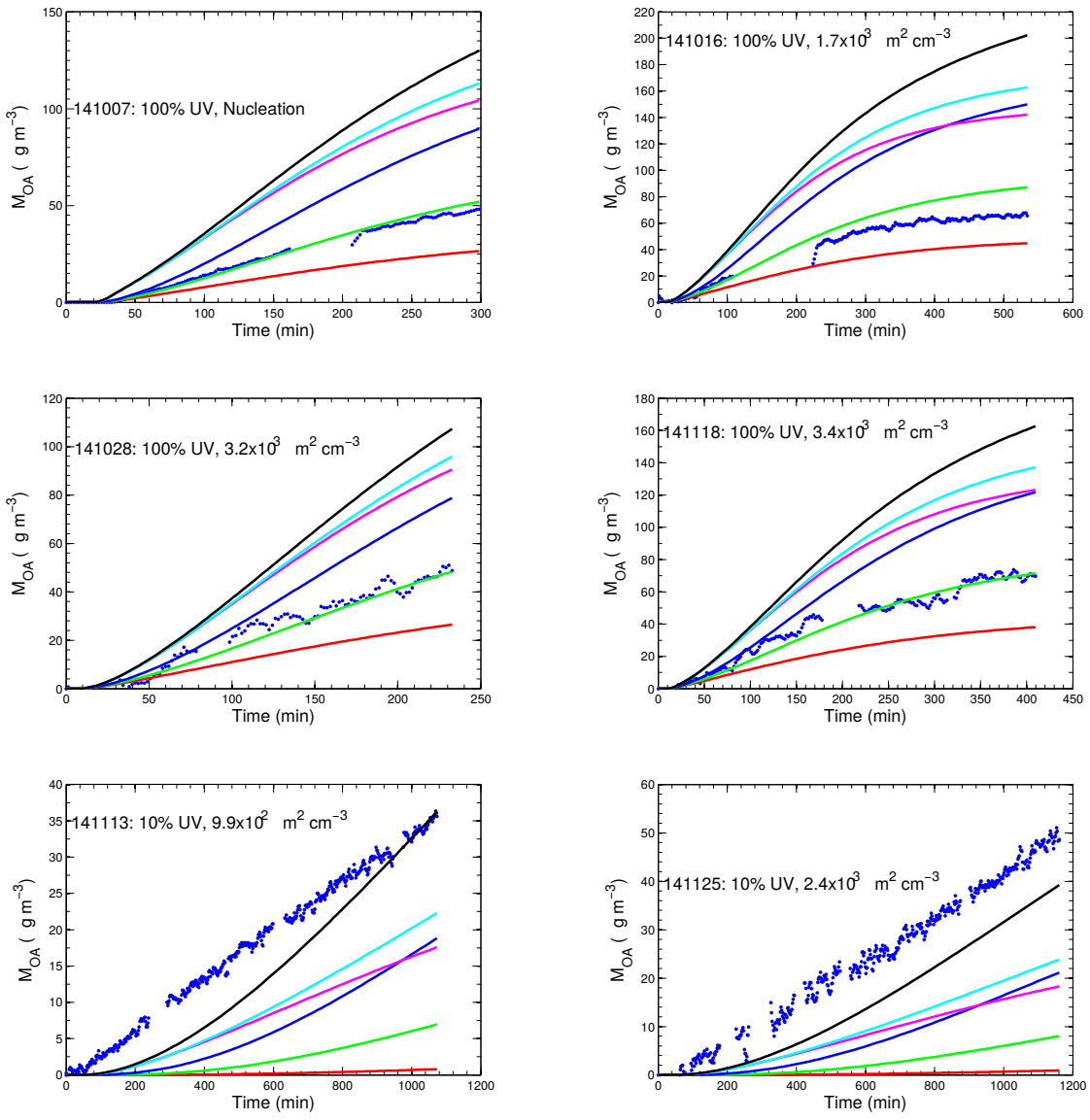

Figure S7: Mass of organic aerosol as a function of time. Experimental measurements are shown with blue data points. GECKO-A predictions are shown for different combinations of $C_w/(M_w\gamma_w)$ and the vapor-wall loss rate k_{gw}: Red line: $C_w/(M_w\gamma_w)$x10 and $k_{gw} = 10^{-3}$ s^{-1}; green line: base $C_w/(M_w\gamma_w)$ and $k_{gw} = 10^{-3}$ s^{-1}; blue line: $C_w/(M_w\gamma_w)$x0.1 and $k_{gw} = 10^{-3}$ s^{-1}; magenta line: $C_w/(M_w\gamma_w)$x10 and $k_{gw} = 10^{-4}$ s^{-1}; cyan line: base $C_w/(M_w\gamma_w)$ and $k_{gw} = 10^{-4}$ s^{-1}; and black line: $C_w/(M_w\gamma_w)$x0.1 and $k_{gw} = 10^{-4}$ s^{-1}.

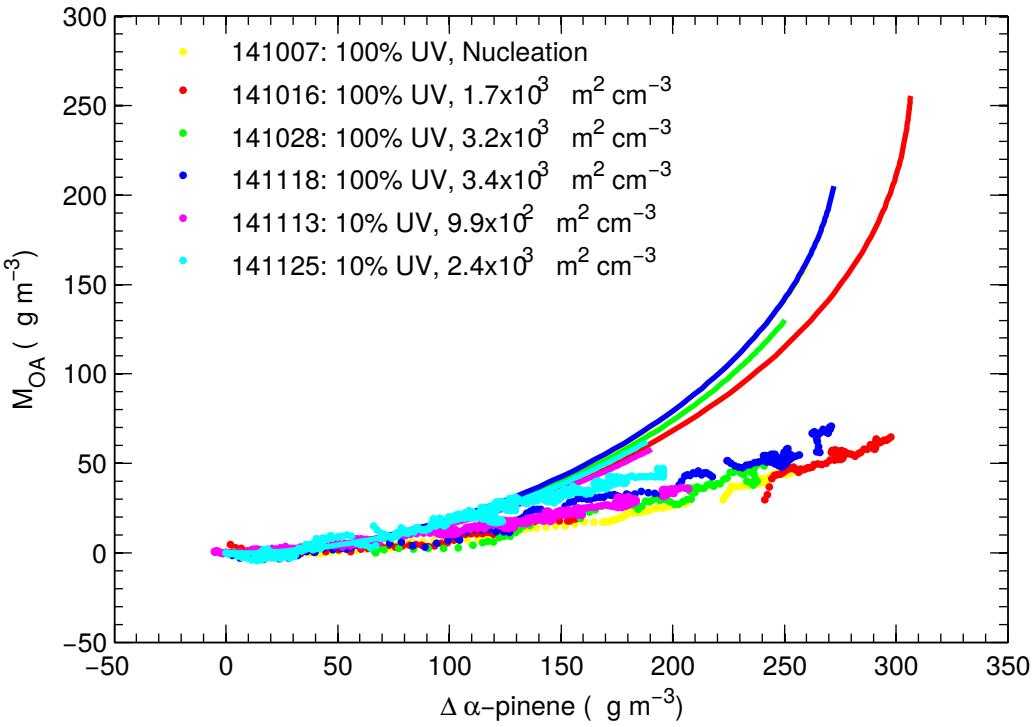

Figure S8: Mass of SOA as a function of reacted α-pinene. Experimental data are shown with filled data points. Solid lines correspond to GECKO-A predictions in the absence of vapor wall loss.

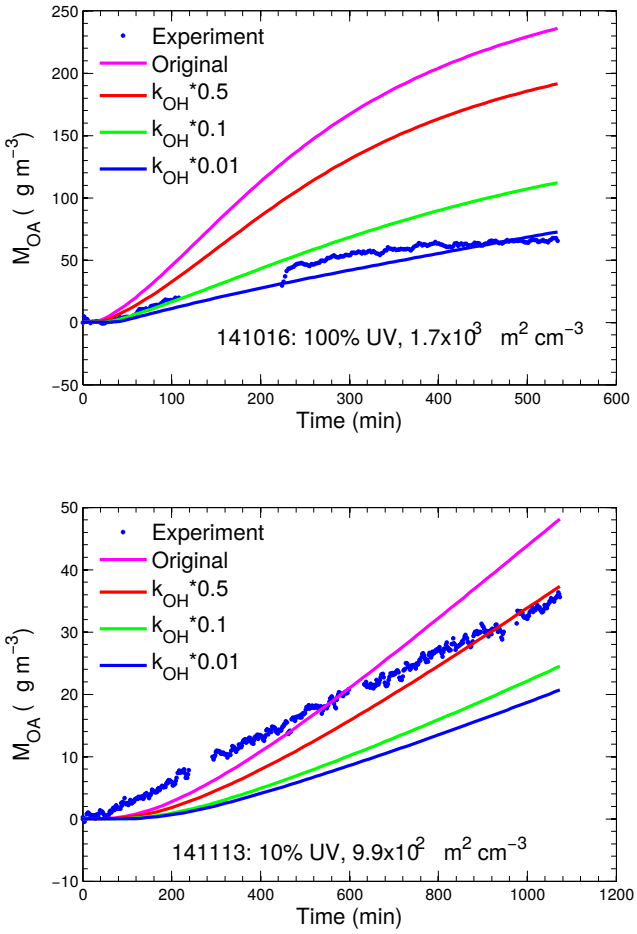

Figure S9: Mass of SOA as a function of time for one high UV and one low UV experiment. Solid lines show GECKO-A predictions with $k_{gw} = 10^{-5}$ s^{-1} and the second and later-generation OH reaction rate constants reduced by varying factors: pink line: no reduction in OH reaction rate constants; red line: OH reaction rate constants reduced to 50% of default values; green line: OH reaction rate constants reduced to 10% of default values; blue line: OH reaction rate constants reduced to 1% of default values.

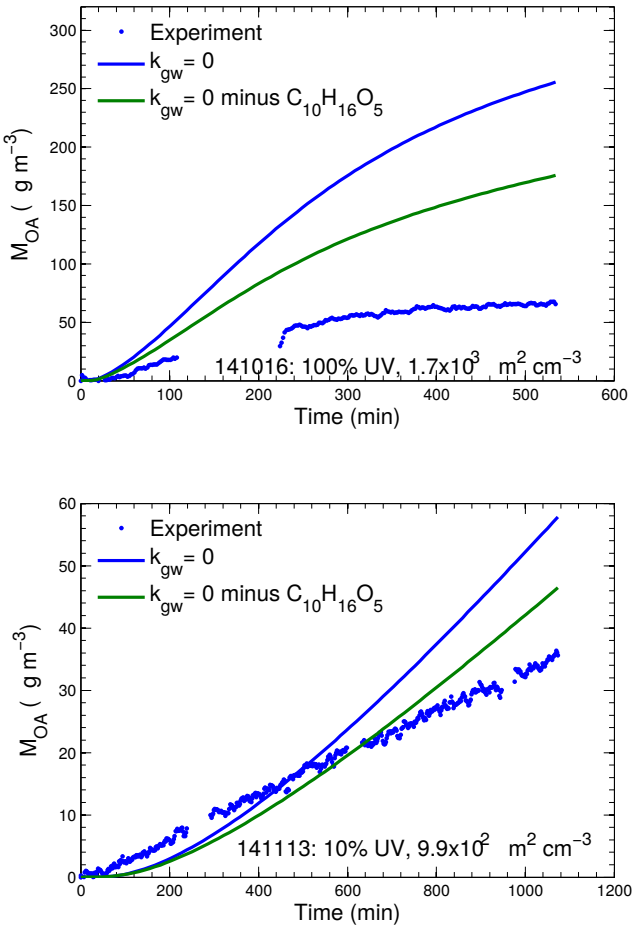

Figure S10: Mass of SOA as a function of time for one high UV experiment and one low UV experiment. GECKO-A predictions simulated with no vapor wall loss are shown by the solid blue line. The green line shows the result of subtracting the α-pinene hydroxy dihydroperoxide, $C_{10}H_{16}O_5$, from the predictions shown with the blue line.

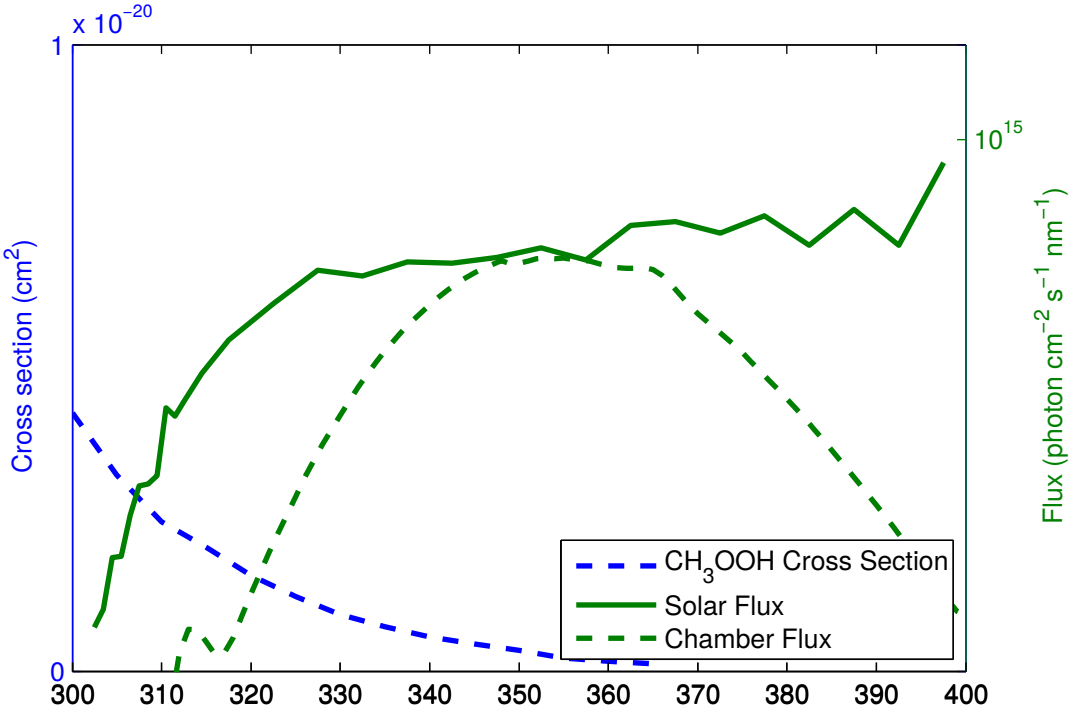

Figure S11: Absorption cross-section of methyl hydroperoxide as a function of wavelength (Sander et al., 2011) compared to photon fluxes of both the sun (Seinfeld and Pandis, 2006) and the Caltech chamber.

References

(1) Pierce, J. R., Engelhart, G. J., Hildebrandt, L., Weitkamp, E. A., Pathak, R. K., Donahue, N. M., Robinson, A. L., Adams, P. J., and Pandis, S. N.: Constraining particle evolution from wall losses, coagulation, and condensation-evaporation in smog-chamber experiments: optimal estimation based on size distribution measurements, Aer. Sci. Technol., 42, 1001–1015, 2008.

(2) Sander, S. P.; Abbatt, J.; Barker, J.R.; Burkholder, J.B.; Friedl, R. R.; Golden, D. M.; Huie, R. E.; Kolb, C. E.; Kurylo, M. J.; Moortgat, G. K.; Orkin, V. L.; Wine, P. H. Chemical Kinetics and Photochemical Data for Use in Atmospheric Studies, Evaluation No. 17. *JPL Publication 10-6*, Jet Propulsion Laboratory, Pasadena, **2011** http://jpldataeval.jpl.nasa.gov

(3) Seinfeld, J. H., Pandis, S. N. *Atmospheric chemistry and physics: from air pollution to climate change*, 2nd ed. Wiley: Hoboken, N.J., 2006.